Proceedings World Geothermal Congress 2020+1
Reykjavik, Iceland, April - October 2021

Using Seismic Interferometry to Identify and Monitor Fluids in Geothermal Systems

Eric Matzel

Lawrence Livermore National Laboratory, Livermore, CA

matzel1@llnl.gov

Keywords: geothermal, interferometry, seismic tomography.

ABSTRACT

Seismic interferometry in combination with waveform modeling is used to measure the seismic properties within geothermal systems, illuminating changes that occur as water moves through the subsurface. I apply "virtual earthquake" methods (ambient noise correlation and active source interferometry) to obtain seismic Green functions (GF) which are then used to calculate material properties, in particular V_S, V_P, Q_S and Q_P. Individually, these properties have complex sensitivity to geologic fabric, composition, and temperature, but in combination they can be used to highlight fractured media through which fluids are transported. In particular, seismic attenuation is highly sensitive to the contrast along fluid filled fractures. Mapping the ratio of the attenuation of P wave energy to S wave energy (Q_P/Q_S) illuminates the fluid paths in the geothermal system. When pressures change, such as during plant operations, fluids move through the system and create measurable changes in the observed amplitudes.

1. INTRODUCTION

The key goal of this study is to understand how fluids travel along faults and fractures through geothermal reservoirs. I focus on two geothermal sites in Nevada: the Brady geothermal field, which was the subject of a multiphysics poroelastic tomography experiment (PoroTomo) (Feigl et al., 2017), and the Blue Mountain geothermal field which has been the subject of several geophysical studies over the last decade, including gravity, magneto-telluric, seismic reflection and refraction surveys.

The PoroTomo site was a 1500-by-500 meter natural laboratory at the EGS field at Brady Hot Springs (figure 1). It was located just north of an existing seismic network run by Lawrence Berkeley National Lab (LBNL) and adjacent to highway I-80. The LBNL network includes 16 three-component 4.5 Hz seismometers sampling continuously at 500 Hz. The experimental phase of the project took place over 15 days in March, 2016. During the PoroTomo deployment, 238 three-component geophones recorded data continuously, and recorded several local and regional earthquakes, vibroseis sweeps, and local traffic noise, as well as the ambient seismic wavefield. In collaboration with Ormat, pumping operations were changed in stages during the experiment. This produced measurable effects on the recorded data. The vibroseis sweeps were performed at points surrounding and within the natural lab, and repeated at identical source points during each of the four stages of operation.

The Blue Mountain geothermal site in northern Nevada included several sets of seismic data in the analysis, involving 3 deployments (figure 2). The first is data from the active source seismic study conducted by Optim in 2007 and used to develop conceptual thermal models of the area (Casteel et al. 2008, Melosh et al., 2010). This involved seven lines, consisting of between 117 to 179 channels along a total of almost 21 miles, and provides nearly 63,000 waveforms. I used these data to create high resolution 2D imagery along each of the 7 transects. The second deployment is a monitoring network deployed by AltaRock, which has been recording continuously since. This network includes 8 contemporaneous 3-component instruments. Originally deployed in late 2015, this network was optimized in October 2016, and two of the stations were relocated to provide higher sensitivity to the local microseismicity. The third deployment was a temporary network set up by Sandia National Laboratory (SNL) which recorded several weeks of continuous data between December 2017 and January 2018 (Poppeliers and Knox, 2017). The combined SNL and AltaRock networks were used to create a local 3D seismic model.

In this paper I discuss the use of seismic interferometry to image the physical properties of the subsurface. These images help capture the detailed changes in velocity and attenuation that may indicate permeable zones and potential drilling targets.

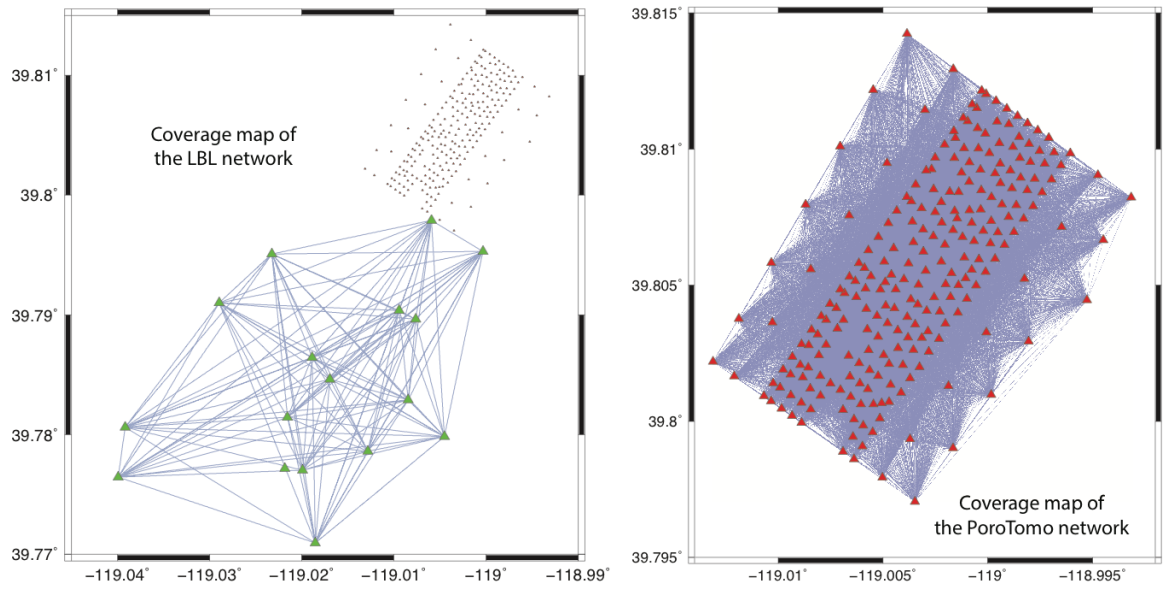

Figure 1: Coverage maps of the Brady Hot Springs. (Left) The LBNL seismic stations (green triangles) lie just south and west of the natural lab. Interferometry allows measurement of the physical properties along paths connecting each pair of seismic stations (blue). (Right) Focusing in on the natural lab site: 238 geophones (red triangles) recorded data during the 15 days of the experiment. The coverage between elements of the natural lab is significantly denser than that of the permanent array.

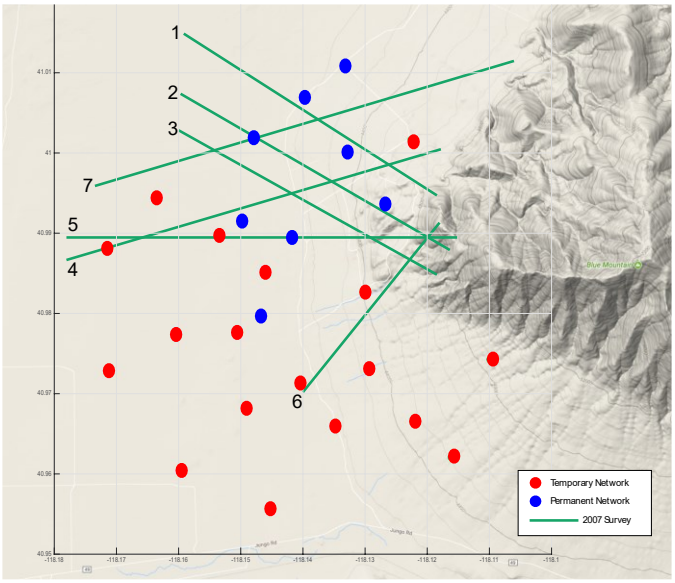

Figure 2: Seismic survey lines (green) and locations of the Blue Mountain temporary (red) and long-term (blue) seismic networks overlaid on topography (from Incorporated Research Institutions for Seismology).

2. SEISMIC INTERFEROMETRY

Seismic interferometry allows precise measurements of the physical properties of the Earth. “Virtual earthquake” methods involve correlating the data recorded at one seismometer with the data recorded at a second to obtain an estimate of the Green function (GF) between the two. A major advantage of virtual earthquake techniques is that there is perfect knowledge of all location and timing constraints, since they are tied to the instruments. In traditional earthquake seismology, uncertainties in the origin time, location and source mechanism of the events have the effect of blurring resolvable images. Interferometry allows high resolution imagery beneath dense seismic networks. Only the structure between the instrument-pair contributes to the signal and even subtle differences in the observed waveforms are valuable for measuring physical properties. Networks can be easily designed to the problem in question, and the resulting GFs are stable enough that 4D variations can be interpreted as changes in subsurface structure.

2.1 Ambient Noise Correlation (ANC)

Ambient noise correlation (ANC) is based on the observation that the Earth's background noise includes coherent energy, which can be recovered by observing over long time periods and allowing the incoherent energy to cancel out (Hennino et a., 2001; Weaver and

Lobkis, 2001). The cross correlation of ambient noise between a pair of stations results in a waveform that is identical to the seismogram that would result if an impulsive source located at one of the stations was recorded at the other (Campillo and Paul, 2003; Malcolm et al., 2004; Snieder, 2004; Wapenaar 2004). Ambient noise correlation has the advantage that it is entirely passive. The disadvantages are that there is little control over the frequency content, which is determined by the natural background field, and the method typically requires long, continuous data records. ANC becomes computationally expensive for high-frequency, large-N data sets.

At Blue Mountain, combining the 18 Sandia instruments with the 8 contemporaneous instruments of the AltaRock network, provided a small network that allowed calculation of a coarse 3D model, which is particularly useful for locating the microseismicity induced by activities at the plant. From the ambient noise, GF for 325 unique paths were calculated crossing the site, giving 250 m resolution laterally to depths of 3 km below the free surface.

The density of instrumentation at Brady allowed significantly higher resolution of the subsurface. Prior to the deployment of the PoroTomo geophone network, 3 months of continuous data recorded at the LBNL network were collected to test the effectiveness of using the ambient noise methodology in the region. Later applied this approach was applied to the 15 days of data recorded by the PoroTomo geophone and DAS networks, as described by Zeng et al. (2016; 2017).

Using data from the LBNL network, I was able to obtain high SNR GF with as little as 24 hours of recorded data. When the full data set is included, I recover high SNR up to 30 Hz. Based on this data set, I created a preliminary seismic velocity model of the site, which allowed prediction of the lateral and depth resolution of the experiment. The dense network at the natural lab increases lateral resolution by more than three orders of magnitude. At the LBNL network, 16 active seismometers provide 120 unique paths over an area of roughly 7.5 km^2. At the natural lab, using data from the 238 geophones, results in 28,203 unique paths sampling an area of 1.5 km^2. At the LBNL network this enables measurement of the variability in the subsurface to depths exceeding 2 km. The PoroTomo resolution extends to depths of several hundred meters.

Because the PoroTomo network was only in place for 15 days, the resulting GF are noisier, particularly at offsets larger than 500 m, and most of the energy is concentrated below 5 Hz. Because the method results in nearly $N^2/2$ GFs, ANC rapidly becomes a “Big Data” problem for large arrays sampled continuously at high frequency and for long periods of time. This makes the calculation computationally expensive. The problem is typically dealt with either by using high performance computers, subsetting the dataset, or prefiltering the raw data and reducing the sample rate.

The “Big Data” problem is addressed by testing a different form of interferometry, described below, that takes advantage of the vibroseis sweeps that were performed during the experiment.

2.2 Active Source Interferometry (ASI)

The second form of seismic interferometry uses the energy of active sources to obtain the GF more quickly, allowing use of records from temporary seismic arrays including reflection and refraction experiments, which are typically much more densely instrumented than long-term monitoring networks. At Blue Mountain, the active source data resulted in significantly higher resolution along the 7 discrete transects. With nearly nearly 63,000 waveforms it is possible to resolve details about 30 m laterally with similar increases in resolution with depth. The tradeoff is that there is no resolution off-axis.

During the PoroTomo experiment, a series of vibroseis sweeps were performed at points surrounding and within the site. These sweeps were repeated at the same points in each of the four phases of the experiment, allowing a search for changes in the material properties over time. For interferometry, the vibroseis sweeps that were performed at points surrounding the site during the experiment are used. In this case, only short records of the active sweeps are required to estimate high frequency GFs. It is computationally much less expensive than ANC, but it is operationally more expensive, since it requires the use of a vehicle with a trained operator. The spectrum of the ASI is determined by both the energy content of the active signals (up to 80 Hz) and the attenuation and propagation properties of the subsurface. Typically, coherent energy up to 30 Hz was recovered. ASI achieves much higher SNR and frequency content using significantly less data (40 minutes total record per stage at PoroTomo) than required by ANC (days). The computational effort becomes much more tractable.

3. WAVEFORM MODELING

I perform a full waveform inversion of the GF data, jointly solving for seismic velocities (V_S and V_P) and attenuation (Q_S and Q_P). The initial objective is to obtain the best fitting 1D model for each trace, the results of which are then combined to create the image of the subsurface. At Blue Mountain, the result is 7 independent 2D tomographic slices along each of the active source lines as well as a lower resolution 3D model that incorporates the results of the others. Using the dense geophysical data sets available at the Blue Mountain geothermal site enables high resolution imagery and association of seismicity with operational changes. By jointly inverting for several geophysical variables, structural interpretations are possible. While individually these parameters have a complex relationship to geology, temperature and composition, in combination they can illuminate fundamental structures. A hot, fractured, porous, fluid-filled media will be characterized by low V_S, low V_S/V_P and high attenuation (low Q) relative to its surroundings. Combining the measures highlights the conductive fractures. In figure 3, I map V_S*V_S/V_P*Q_S from the inverted model. The low valued (red) portions of the image follow the known geologic faults, supporting the conceptual model of Melosh that fluids flow up along the fault surfaces and down along the contact at the edge of the mountain.

Matzel.

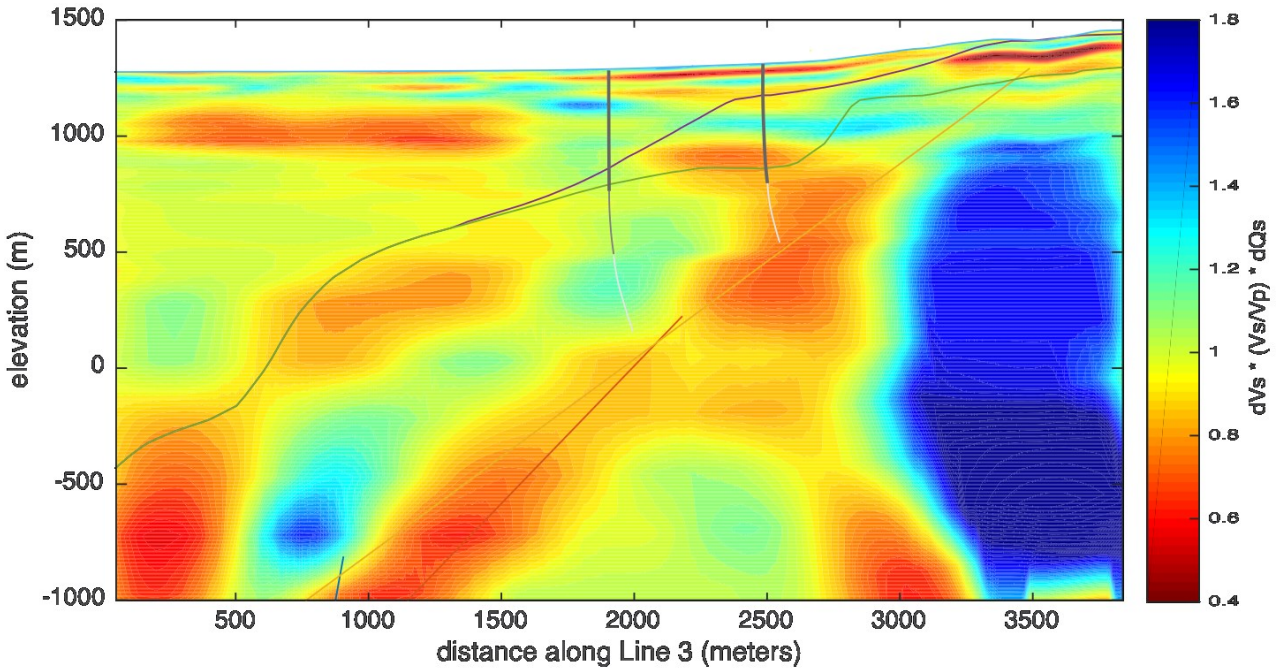

Figure 3: Combining measurements illuminates the geothermal system along Blue Mountain seismic line 3. Hot, fractured, porous, fluid-filled media are characterized by low VS, low VS/VP and high attenuation (low Q) (red colors) relative to their surroundings. Major faults and contacts from the geologic reference model are superimposed as lines.

At Brady, I inverted the ASI waveforms from the surface to 1 km depth to create a 3D model of the natural laboratory. Low shear velocities align with mapped hot-spots including fumaroles and with faults. V_P/V_S is very high and laterally heterogeneous at the surface ranging between 3-6, with the highest near the faults and hotspots. V_P/V_S drops rapidly as a function of depth in the top 100 m. Attenuation is also very high near the mapped hot spots and fumaroles.

An intriguing result of that work is that the ratio Q_S/Q_P appears to be highly sensitive to the presence of the injection fluids. In most elastic geological materials, shear waves are more highly attenuated than pressure waves ($Q_S < Q_P$). In fractured or porous materials, this relationship changes. Shear waves can't travel through acoustic media, like gas or fluids, traveling only through the solid matrix surrounding them. Compressional waves travel through both acoustic and elastic media and are able to sense the difference between fully and partially saturated media. In these environments, Q_S can often be larger than Q_P and the ratio (Q_S/Q_P) can be used to map the fluids in the subsurface. Mapping the Q_S/Q_P ratio (figure 4), we can see strong correlation with the location of fluid injection and the geothermal fumaroles.

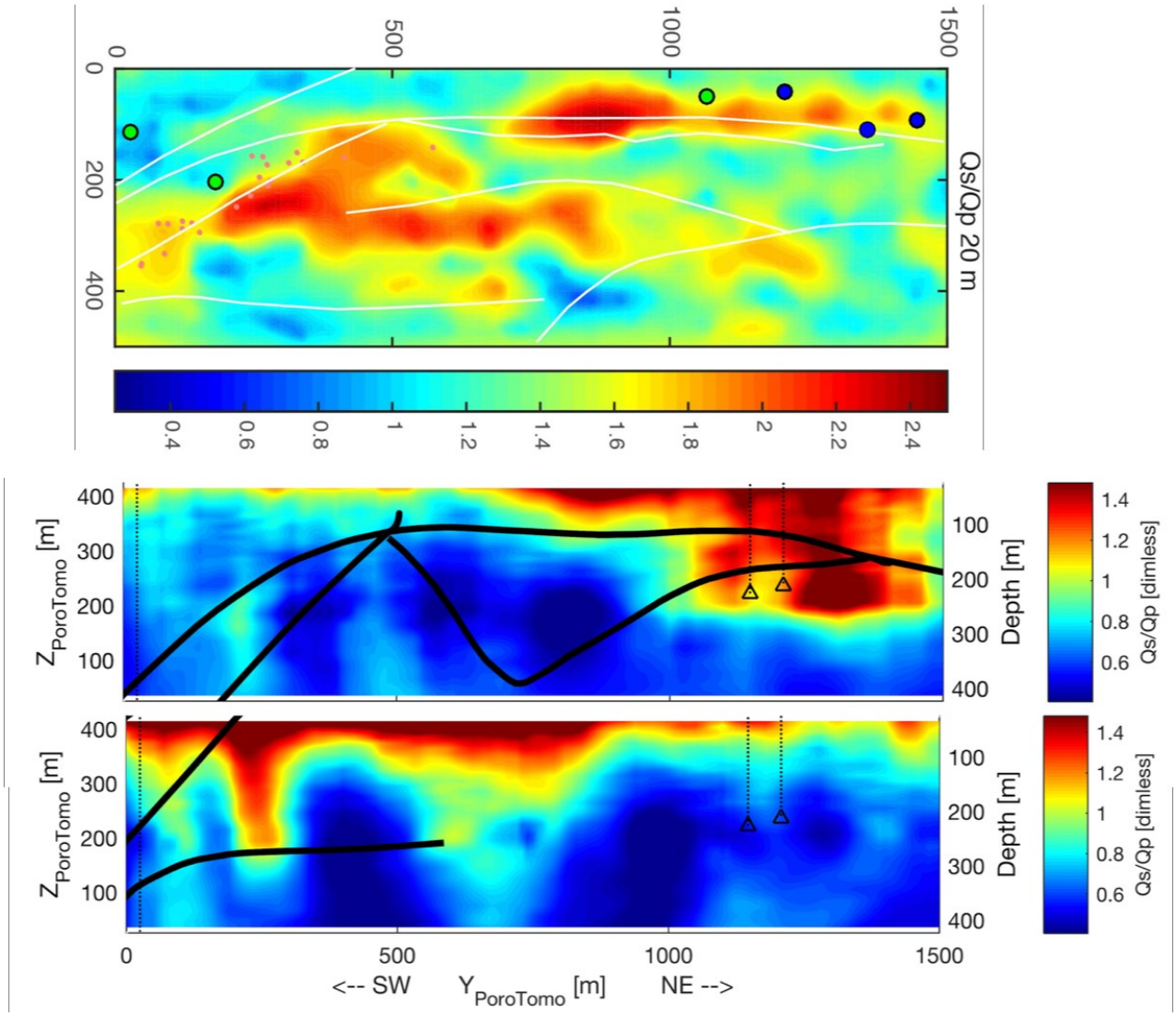

Figure 4: Q_S/Q_P illuminates fluid pathways at the Brady geothermal site. (Top): map view of Q_S/Q_P at 20 meters below the surface, with plotted injectors as blue circles and monitoring wells as green circles. Cross-sections through the injection point (middle) and the fumaroles (bottom). High Q_S/Q_P (redder colors) correlate strongly with areas known to have high fluid flow. Major faults and contacts from the geologic reference model are superimposed as lines.

4. CONCLUSION

I use data from a pair of geothermal sites to study the capabilities of seismic interferometry for resolving physical structures, in particular, the locations of faults and fractures that serve as pathways for fluid transport. Using a combination of active and passive seismic interferometry, I am able to resolve highly heterogeneous structures. At both Brady and Blue Mountain, highly attenuating low shear velocity regions are correlated with the flow paths of fluids in the geothermal systems. Seismic velocities (V_S and V_P) and attenuation (Q_S and Q_P) are measured, each of which have different sensitivities to the presence of fluids, fractures and temperature. Absolute velocities highlight compositional variations. Ratios of V_S to V_P emphasizes changes in material properties such as porosity. Attenuation of seismic energy is observed to be high in locations known to be hot and heavily fractured. Combining measurements illuminates the geothermal system including the fluid flow paths. Hot, fractured, porous, fluid-filled media are characterized by low V_S, low V_S/V_P and high attenuation (low Q) relative to its surroundings, while the ratio Q_S/Q_P is particularly sensitive to fluid saturation.

This work performed under the auspices of the U.S. Department of Energy by Lawrence Livermore National Laboratory under Contract DE-AC52-07NA27344, with funding from the Geothermal Technologies Office.

REFERENCES

Campillo, M., and Paul, A.: Long-range correlations in the diffuse seismic coda: Science 229, (2003), 547–549.

Casteel, J., Melosh, G., Niggemann, K. and Fairbank, B.: Blue Mountain Step-Out Drilling Results. Transactions, Geothermal Resources Council, (2008).

Feigl, K. L., and PoroTomo_Team: Overview and Preliminary Results from the PoroTomo Project at Brady Hot Springs, Nevada: Poroelastic Tomography by Adjoint Inverse Modeling of Data from Seismology, Geodesy, and Hydrology, paper presented at Stanford Geothermal Workshop, Stanford University, (2017).

Matzel.

Hennino, R., Tregoures, N., Shapiro, N.M., Margerin, L., Campillo, M., van Tiggelen, B.A. & Weaver, R.L.: Observation of equipartition of seismic waves, Physical Review Letters, 86, (2001), 3447-3450.

Malcolm, A.E., Scales, J.A. & van Tiggelen, B.A.: Extracting the Green function from diffuse, equipartitioned waves, Physical Review E, (2004), 70.

Melosh, G., Cumming, W., Casteel, J., Niggemann, K. and Fairbank, B.: Seismic Reflection Data and Conceptual Models for Geothermal Development in Nevada, Proceedings World Geothermal Congress (2010).

Poppeliers, C. and Knox, H.: Moment tensor inversion, perforation. International Federation of Digital Seismograph Networks. Other/Seismic Network. (2017), 10.7914/SN/X9_2017

Snieder, R.: Extracting the Green's function from the correlation of coda waves: a derivation based on stationary phase, Physical Review E, (2004), 69, 046610.

Wapenaar, K.: Retrieving the elastodynamic Green's function of an arbitrary inhomogeneous medium by cross correlation: Physical Review Letters, 93, (2004), 254301.

Weaver, R. L., and O. I. Lobkis, 2001: Ultrasonics without a source: Thermal fluctuation correlations at MHz frequencies: Physical Review Letters, 87, (2001), 134301.

Zeng, X., C. Thurber, H. Wang, D. Fratta, E. Matzel, and PoroTomo_Team (2017): High-resolution Shallow Structure Revealed with Ambient Noise Tomography on a Dense Array, paper presented at Stanford Geothermal Workshop, Stanford University (2017).

Zeng, X., C. Thurber, Y. Luo, E. Matzel, and PoroTomo_Team (2016): High-resolution shallow structure revealed with ambient noise tomography on a dense array (abstract #S13B-2574), in Fall Meeting Amer. Geophys. Un., edited, AGU, San Francisco (2016).